PROCEEDINGS OF SPIE

SPIEDigitalLibrary.org/conference-proceedings-of-spie

Design of a multi-element FSO transceiver array for mobile communication links

De La Llana, Patrick, Haq, A F M Saniul, Yuksel, Murat

Patrick N. De La Llana, A F M Saniul Haq, Murat Yuksel, "Design of a multi-element FSO transceiver array for mobile communication links," Proc. SPIE 11678, Free-Space Laser Communications XXXIII, 1167805 (10 March 2021); doi: 10.1117/12.2582633

SPIE.

Event: SPIE LASE, 2021, Online Only

Design of a multi-element FSO transceiver array for mobile communication links

Patrick N. De La Llana[a], A F M Saniul Haq[b], and Murat Yuksel[a,b]

[a]Department of Electrical and Computer Engineering, University of Central Florida, FL USA
[b]The College of Optics and Photonics, CREOL, University of Central Florida, FL USA.

ABSTRACT

Free-space optical communication (FSOC) have directional light beams which makes communication links very sensitive to movement. A major challenge in mobile settings is handling of this fragility of FSOC links due to the highly directional distribution of light intensity within the light beams. Differing from previous studies using mechanical steering of the transceivers to remedy the brittleness of FSOC links, we use a square array of stationary elements for each transceiver for better directionality, optimum combination of elements (transmitter/receiver ratio along with location), and robustness to mobility. Based on previous studies showing the optimum transmit to receive area ratio in a square array layout, we locate the transmitters as a box around the center with extra elements on the four corners of the transceiver plane with the rest of the elements on the array being receivers. We design a hardware prototype using the same optimum transmit/receive ratio and a 10x10 square array layout with size, weight and power, cost, and geometric simplicity appropriate for a low-flying multi-copter drone. A full link margin analysis was completed for the 10x10 array, using commercial off-the-shelf components, with the same optimum transmit and receive combination. The range for the system was found to be $\sim$ 150 m operating at 1 Mbps. The outcome of this work will give us insight of how the tiling of transmit/receive elements affects a transceiver system to implement a directional wireless link in the optical spectrum for mobile settings, particularly for emerging use of low-flying drones.

Keywords: FSO, Optical Transceiver, Link Margin

1. INTRODUCTION

Free space optical communication (FSOC) utilizes the optical spectrum rather than the commonly used and overly saturated radio frequency (RF) spectrum. As the legacy RF band is being over-crowded with the enormous data demand, alternate bands such as optical and millimeter wave (mmWave) are becoming popular for next generations of wireless networks. With the fiber optic backhaul network, optical bands present the opportunity to satiate the data demand by complementing existing legacy RF network and utilize the full potential of the system.[1,2] FSOC can provide high speed networking with faster modulation speeds, broader bandwidth, secure directional beam steering, and utilization of unlicensed spectrum.[3] Semiconductor light sources, such as light emitting diodes (LEDs) and lasers, may provide low cost, compact, and energy efficient high speed communication system for mobile applications. Even though the requirement of direct line-of-sight (LOS) and weather-dependent propagation loss limit the link range of the system, FSOC offers the promise to be the solution for futuristic smart cities and other terrestrial applications. Tactical ad-hoc network that requires high bandwidth and low probability of interception can be implemented with the use of FSO transceivers. On top of that, the network capacity can be significantly improved by implementing FSO transceivers in an in-band full-duplex (IBFD) configuration.[4] Despite the disadvantages caused by self-interference (SI), full-duplex operation can increase channel capacity which is essential for the huge data demands.[5]

Further author information:
Patrick De La Llana: E-mail: patrickdelallana@knights.ucf.edu
A F M Saniul Haq: E-mail: saniul.haq@knights.ucf.edu
Murat Yuksel: E-mail: murat.yuksel@ucf.edu

Free-Space Laser Communications XXXIII, edited by Hamid Hemmati, Don M. Boroson, Proc. of SPIE Vol. 11678, 1167805 · © 2021 SPIE
CCC code: 0277-786X/21/$21 · doi: 10.1117/12.2582633

The FSO beams exhibit a very skewed distribution of light intensity following the Lambertian Law,[6] which makes the communication link very sensitive to movement. Most of the literature on mobile FSOC considered mechanical steering of transmitter and/or receiver for pointing and acquisition of the brittle link.[7] Redundancy of transceivers on a mobile platform was also explored to tackle the LOS alignment challenge.[8] In this paper, avoiding the main limitations of mobile FSOC, which include LOS blockage, absorption, and atmospheric attenuation, we design a transceiver circuit that uses FSO as a means of wireless data transmission to demonstrate the use of a transceiver system using FSO arrays with multiple transmitters and receivers. In particular, we focus on the tradeoffs in the size, weight, and power (SWaP) of the transceiver against the budget of the mobile FSOC link, for which we use the SWaP constraints as a list of digital communication design objectives.[9]

To improve link quality and ensure higher throughput, multi-element design can be implemented for directional FSOC.[10,11] A preceding study of ours on the optimum combination and placement of the elements on the arrays provided us a guideline of designing multi-element FSO transceiver module. The study analyzed both optimum number of transmitters and receivers, and their placement and numerical combination on the FSO transceiver array. It is found from simulation that on a 100x100 square array of elements, the optimum transmit/receive ratio was 2,200 transmit elements and 7,800 receive elements, and optimum transmit/receive layout is transmitters located as a box around the center with extra elements focused on the four corners of the box, while the rest of the elements on the square array were receive elements. We design and analyze a FSO transceiver circuit using the same optimum transmit/receive ratio and layout with a 10x10 square array (imitating the 100x100 square array with a smaller size due to compactness, cost, and simplicity) and consider placement of both onto low-flying drones. The same optimum ratio and layout of the simulation of the 100x100 array will be used for the 10x10 array. Using a data rate of 1 Mbps will give proof that the array will be able to transmit and receive significant information to be considered successfully demonstrated. The future goal is to fully design a transceiver system for drones using the 10x10 or larger array to demonstrate the theory of the study and give real results. This paper presents a precursor to this goal.

In this paper, we maximize the performance of the optical wireless system by optimizing the circuit components of the transceiver. We explore the effect of multi-elements in the circuit and how the multi-element design can impact the performance of the overall system. The main contributions are as follows:

- A model of the FSOC link is developed and used to perform link margin analysis for optimizing the link range for a given system of multi-element transceiver.
- An optimized approach to design the transmit and receive circuit to obtain the best performance from the overall system, while maintaining SWaP conditions.
- An integrated prototype design of the transceiver circuit to demonstrate the effectiveness of the designed circuit.

The explanation and review of the design are organized as follows: Section 2 discusses the channel performance and factors driving the system requirements, and also derives and explains the equations used for the link margin analysis. From the equations alone, it may not be clear of what specific aspect will drive system performance. Hence, Section 3 summarizes the results of the link margin, which gives a clear picture to what are the most important factors that drive the system performance. Given the link margin analysis, Section 4 explains circuit design criteria and considerations. We conclude the paper with a summary of the results and future research prospects.

2. CHANNEL PERFORMANCE ANALYSIS

In any communication analysis and design, the first step is always to do the link margin or budget analysis. The link margin analysis is the driver behind the requirements for any communication system since. Much of the knowledge in communications analysis and hardware design that is used in the RF spectrum is also applicable in the optical spectrum. A major example is how link margin analysis is done for any communication system, regardless of what spectrum the frequency is in. Receiver sensitivity, noise figure analysis, gain, free-space loss, and many other parameters are typical parameters that are used in both RF and optical communications analysis.

In the following, we describe, for a typical FSOC system, the derivation and explanation of the equations used for the system design and analysis.

2.1 Channel Propagation Model

The first major step is to show the derivation of the Friis equation for power transmission.[12,13] We consider an isotropic point source radiating equally in all directions, which is in the shape of a sphere. Since the area of a sphere is the direction of the transmission of energy in an isotropic point source, the surface area of the sphere is used for the spread of the signal, a.k.a. the power density:

$$\frac{P_t}{\text{Surface Area}} = \frac{P_t}{4\pi R^2} \tag{1}$$

where P_t is the transmit power at the source, and R is the communication range corresponding to the radius of the sphere. After including associated transmit, G_t, and receive, G_r gains of the transmitter and receiver systems into (1), we can write the received power, P_r, as follows:

$$P_r = \frac{P_t G_t G_r A_e}{4\pi R^2} \tag{2}$$

where the effective aperture of an isotropic antenna, A_e, is on the receiver side, which is derived using the thermodynamic argument and Ray-Jeans Law.[14] The thermodynamic argument has the following true:

$$P_A = P_J \tag{3}$$

where P_A is the power received by the antenna at a particular temperature T and range of frequencies Δf. P_J is the Johnston-Nyquist noise power by the resistance at temperature T and range of frequencies Δf, and is given by the following:

$$P_J = KT\Delta f. \tag{4}$$

where $K = 1.381\times10^{-23}$ J/°K is Boltzmann's Constant P_A is found to be the following for an isotropic radiator:[14]

$$P_A = A_e B_A \Delta f \frac{1}{2}\int_0^{4\pi} d\Omega = 2\pi A_e B_A \Delta f \tag{5}$$

The Ray-Jeans Law is an approximation of black-body radiation, B_A, as a function of wavelength at any given temperature. In the RF range, it is correct to assume the black-body radiation to be given by the Ray-Jeans Law, which yields the following:[14]

$$B_A = \frac{2KT}{\lambda^2} \tag{6}$$

where λ is the wavelength (m). Plugging in (5), (6), and (4) into (3) yields A_e as follows:

$$2\pi A_e \frac{2KT}{\lambda^2}\Delta f = KT\Delta f \tag{7}$$

$$A_e = \frac{\lambda^2}{4\pi}. \tag{8}$$

The effective aperture, and associated gains and losses with the transmit and receive system yield the following for the final derivation of the general isotropic Friis equation:[14]

$$P_r = \frac{P_t G_t G_r \lambda^2}{(4\pi R)^2} \tag{9}$$

Since our system is using optical signal transmission, the final P_r will not be the same as the isotropic derived P_r, with the actual equation used for analysis shown below. The generalized Friis equation for optical communications[15] was derived from the Friis equation above to be the following:

$$P_r = P_t G_t G_r T_{a_t} L_{F_S} \tag{10}$$

$$L_{F_S} = \frac{\lambda^2}{4\pi} \frac{A_R}{2\pi R^2(1 - cos\theta)} \tag{11}$$

$$T_{a_t} = e^{-\alpha R} \tag{12}$$

where θ is the beam divergence angle from the light source, P_t is the transmit power in Watts, A_R is the surface area of the optical receiving component region (in our case the absorbing part of the photodiode). This differentiates from the effective area A_e as the effective area is the electromagnetic receiving area of an assumed isotropic antenna while A_R is just the surface area of the optical receiving component region. L_{F_S} represents the free-space loss, and T_{a_t} represents the atmospheric loss. The term α is the atmospheric attenuation coefficient, which is calculated using the equation below:[3]

$$\alpha = \frac{3.91}{V} \left(\frac{\lambda}{550 \times 10^{-9}} \right)^{-q}, \tag{13}$$

where V is the visibility (km), and q is calculated using the following parameters below:

$$q = \begin{cases} 1.6; & V > 50 \text{ km} \\ 1.3; & 6 \text{ km} < V < 50 \text{ km} \\ 0.72V^{\frac{1}{3}}; & V < 6 \text{ km}. \end{cases} \tag{14}$$

The version of P_r shown in (10)-(12) is used for calculating the received carrier power in our analysis.

2.2 Link Performance Model

As a measure of performance, we focus on the Signal-to-Noise Ratio (SNR) as the attribute representing the signal fidelity of a FSOC system. The SNR is of utmost importance when doing the link margin analysis, as the link margin calculation is mostly the SNR with all the associated gains and losses. The total noise power of the system (also known as the receiver sensitivity, which is the smallest signal a receiver can detect) is defined as the following:[16]

$$N = KTB \text{ Req}\frac{P_r}{N} \tag{15}$$

where T is system temperature (°K), B is the system bandwidth (Hz). $\text{Req}\frac{P_r}{N}$ is defined as the required SNR component of the system, which is a characteristic of the receiver in question. The KTB part is considered as the thermal noise power of the system (same as Johnson-Nyquist noise). The receiver sensitivity is the summation of the thermal noise power and the additional receiver characteristics of the system. $\text{Req}\frac{P_r}{N}$ is the required SNR ratio that is characterized by the design attributes of the receiver. It is defined as the following[16] :

$$\text{Req}\frac{P_r}{N} = \text{Req}\frac{E_b}{N_0}\frac{R_b}{B_e} \tag{16}$$

where B_e is the equivalent noise bandwidth of the receiver.[16] Here, N_0 is the noise density and has the following relationship:

$$N_0 = KT \tag{17}$$

where R_b is the bit rate in bits per second. $\text{Req}\frac{E_b}{N_0}$ is the energy per bit to noise spectral power density ratio, or more commonly known as SNR per bit. This is found from the Bit Error Rate (BER) vs. $\frac{E_b}{N_0}$ curve. Hence, BER is defined as the following:

$$\text{BER} = \frac{1}{2}\text{erfc}\left(\sqrt{\frac{E_b}{N_0}}\right) \tag{18}$$

where erfc(.) is the complementary error function, defined as $\text{erfc}(z) = 1 - \frac{2}{\sqrt{\pi}} \int_0^z e^{-t^2} dt$. Following the typical telecommunication standard of maximum BER of 10^{-9}, we use the BER vs. E_b/N_0 curve for On-Off Keying

(OOK) modulated signal to find the required SNR per bit to be Req$\frac{E_b}{N_0}$ = 13.2 dB. From the previous explanation, the following is the Ifinal link margin (LM) calculation:

$$\mathrm{LM} = \frac{P_r}{NS} \tag{19}$$

where S is the system reserve, which is a preset amount of margin held in the calculation that accounts for component degradation. Converting the LM to dB, this yields:

$$\mathrm{LM} = 10\log\frac{P_r}{NS} = P_r - N - S. \tag{20}$$

3. LINK BUDGET ANALYSIS

By using the designated system parameters discussed in Section 2, we evaluate the link budget of a given FSOC system. In this section, the link margin analysis is done using an array of 100 elements with multiple transmitters and receivers. A key issue is to determine the number of transmitters and receivers on the FSOC transceiver array. In our previous studies, we have found that for FSOC using an array of optical transmit and receive components in a specific set pattern can influence the overall link performance. Hence, the number of transmitters and receivers are determined based on a simulation employing FSO propagation and Signal-to-Interference-plus-Noise Ratio (SINR) calculation for the FSOC between two arrays located on hovering drones. The simulation is performed to calculate the optimum number of transmitters and receivers within an array to maximize SINR of the channel. The simulation was performed for a 100×100 square array with elements assigned to each grid locations, with the goal of finding the optimum locations for transmit and receive elements. For real-world applications, transmit sources would be light emitting components (such as an LED or a VCSEL), while the receive components would consist of photodiodes. First, we calculated the SINR of the link by varying the number of the transmitters to calculate the optimum number of transmitters. Once we calculated the number of transmitters required to maximize the link performance, we randomly generated 350,000 patterns for placing the transmitters in different grid locations. Then, we selected the patterns that have best performances and used those to approximate the optimum locations of the transmitters. The simulation results indicated about 78% area of the transceiver array plane needs to be covered with receivers to achieve the best link performance. In practice, 100×100 array is not practical for implementation, but we used this grid size to achieve finer grid locations, that can give us better view for position determination. By implementing the knowledge gathered from the simulated 100×100 array, we design a 10×10 array transceiver that can feasibly meet SWaP requirements of low-flying drones. For a 10×10 array design, the number of transmitters needs to be 22 and the number of receivers 78 according to the guidance from the simulations. However, to balance the transmitter circuit current for uniformity, we choose a combination of 24 transmitters and 76 receivers for our transceiver array design. We will discuss the details of the electrical circuit design aspect of the transceiver in details in Section 4. We now continue with analyzing the link budget using 10×10 FSO transceiver arrays.

We investigate further to determine the transmit power and beamwidth of the optical transmitters. The link range of the channel increases with higher transmit power (P_t) and smaller divergence angle (θ), as shown in Fig. 1. The increase in transmit power effectively increases the power received by the receivers and gives better link margin. Based on the analysis in the previous section, the equation for link range relation to transmit power is:

$$R = \sqrt{\frac{P_t G_t G_r T_{a_t} \lambda^2 A_R}{8\pi^2 SKTB\mathrm{Req}\frac{P_r}{N}(1-\cos\theta)}} \tag{21}$$

where θ is the divergence angle. As we reduce the divergence angle of the transmitters, the beamwidth of the link becomes more directional and focused, hence increases the power delivered at receiver. This direct relationship can be used to select the components with the best divergence angle, which can be done after rearranging (21):

$$\theta = \arccos\left(1 - \frac{P_t G_t G_r T_{a_t} \lambda^2 A_R}{8\pi^2 SKTBReq\frac{P_r}{N}R^2}\right) \tag{22}$$

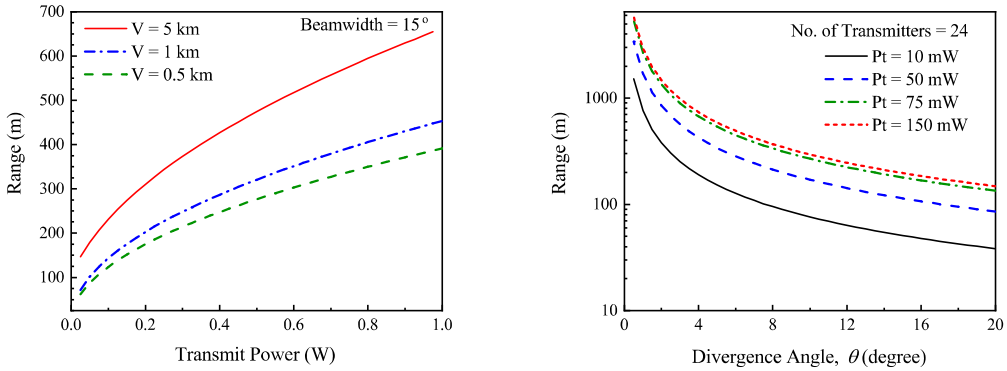

Figure 1. Range calculation for (left) different transmit power for $V = 5$ km, (right) different bit rate with 24 transmitters, each having 75 mW transmit power.

Depending on the atmospheric condition, such as visibility (V), the link range can vary as well. For more clear weather, such as $V = 5$ km, we see a significant improve in link range compared to less clear atmosphere, such as $V = 0.5$ km. We will consider $P_t = 75$ mW and divergence angle $\theta = 15^\circ$ for our further studies as these values represent more practical values for VCSELs available commercially. According to our analysis, the link range for $P_t = 75$ mW and $\theta = 15^\circ$ at clear weather ($V = 5$ km) is 139 m at 1 Mbps. Considering all the constraints and SWaP requirements, we set the system bit rate to 1 Mbps and carrier wavelength of 850 nm. Based on the system parameters and including system reserve of 1 dB, the link margin is calculated to be 4.82 dB for 24 transmitter channel with transmit power of 75 mW each. In order to calculate the maximum bit rate with respect to range, we use the link margin from (19) and the received power from (10), and obtain:

$$R_b = \frac{P_t G_t G_r T_{a_t} \lambda^2 A_R B_e}{8\pi^2 SKTB\frac{E_b}{N_0} R^2 (1 - \cos\theta)} \tag{23}$$

The link range of the channel also depends on the system parameters like bit rate, frequency, and bandwidth. As shown in Fig. 2, link range of the channel drops significantly with the increase of data bit rate. For a clear atmosphere with $V = 5$ km, the link range drops almost 70% if the bit rate is increased from 1 Mbps to 10 Mbps. The effect on link range is even higher if the weather condition deteriorates.

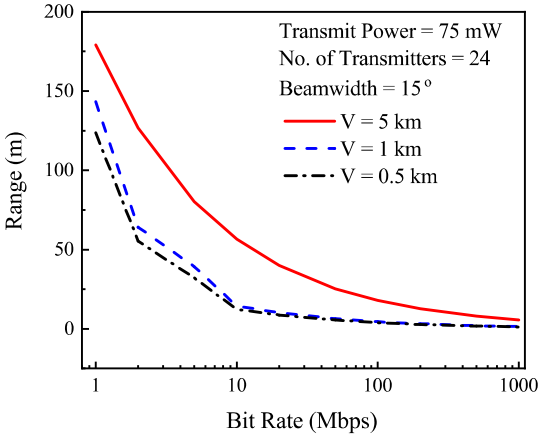

Figure 2. Range calculation for different bit rate with 24 transmitters, each having 75 mW transmit power

The use of optical signal to transmit data enables many advantages, such as higher bandwidth, which ensures the technology can deliver the high data demand. The higher carrier frequency, or smaller signal wavelength, increases available bandwidth to satiate the higher data demand, as shown in Fig. 3. However, smaller wavelength or higher frequency attenuates faster in free space, resulting in much higher free-space loss. Again, overall bandwidth is dependant on transmit power limit as well.

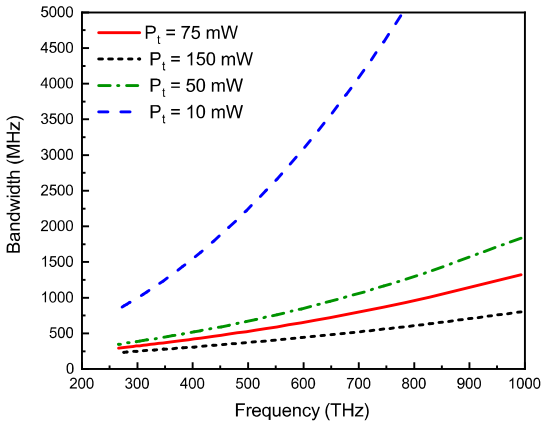

Figure 3. Bandwidth variation with frequency for FSO transceiver.

4. TRANSCEIVER CIRCUIT DESIGN

In this section, we elaborate on our circuit design concepts for the multi-element FSO transceiver. We present how the constraints of SWaP are considered into our design to implement the overall circuit. To design the overall transceiver circuit, we consider the system parameters outlined in the previous section. To layout the system architecture, we need to design two separate circuits within a transceiver, where both of the circuits are controlled with a single controller, e.g. Arduino or Raspberry Pi.

4.1 System Architecture

As outlined in the previous section, the overall system architecture includes 10×10 array with the transmit sources forming an internal box with extra elements on the four corners of the box. The receiver elements are the rest of the elements on the array. The number of transmit sources is 24 and the number of receiver photodiodes is 76. These transmit and receive circuits were routed and simulated separately in the EDA software for simplification. The overall system architecture is shown in Fig. 4. The description of each circuits are presented below.

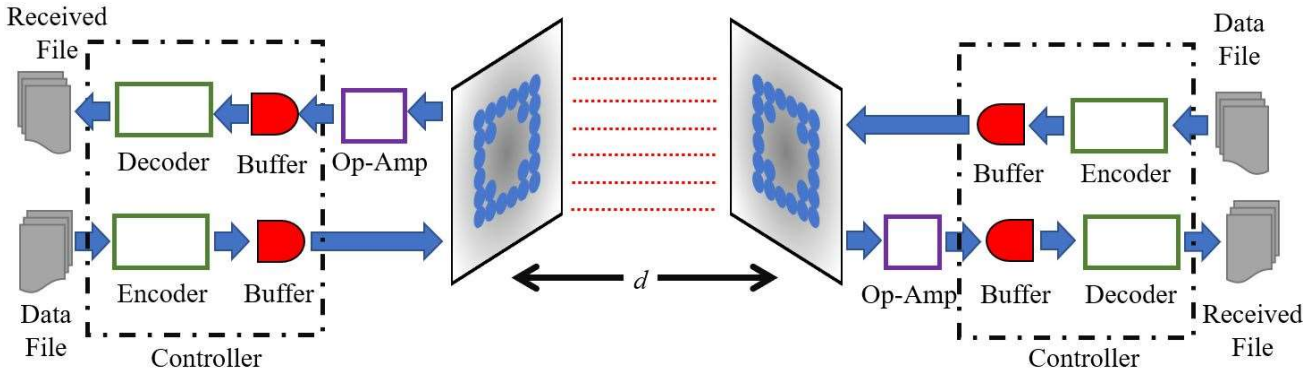

Figure 4. Overall system schematic.

4.1.1 Transmit Path Schematic

As discussed in Section 3, the optical simulation provides the best performance for 22 transmitter for a 10×10 array transceiver plane. However, to attain the required routing path for steady and balanced current for the said 22 transmitters, the necessary voltage source is too big to incorporate within the overall system. The weight, capacity, and cost of the voltage source outweighs the performance improvement achieved. Instead, by using 24 transmitters, we have the options to distribute the transmitter along multiple routes and balance the current supplied to each transmitter.

The layout of the board was chosen for a factor of reasons. To match feasibility (SWaP) and affordability, the design is implemented with a 10×10 array with the same relational geometry between the transmit and receive elements. Of the possible outcomes of the 10×10 design which would designate 76 receivers and 24 transmitters, there were several possible layouts to match these requirements to give correct geometry for the transmit chain. The routing possibilities could have been any of the following format in (elements per path): 24×1, 12×2, 8×3, 6×4. In our design, we chose the 8×3 layout for several reasons. First and foremost, 6×4 and 8×3 were the easiest to design depending on the input supply being a higher voltage or current. For very high frequencies, they would also be easier to design to have the least amount of lag and difference in between transmission time for each of the individual elements. The important factor in this regard is what each individual LED/VCSEL transmits, as the combination of all the transmitting elements' aggregate power will give a better SNR for the receiving end. By ignoring resistance noise (since very low resistance values are used for this design), the high power transmitted for each element will allow the SNR to be better. The second reason why the 8×3 layout was chosen due to voltage and current driving requirements of the transmitter circuit elements (narrow band LEDs). The lowest amount of weight for SWaP for voltage and current driving requirements was most easily met with the 8×3 layout. The transmit circuit schematic is shown in Fig. 5

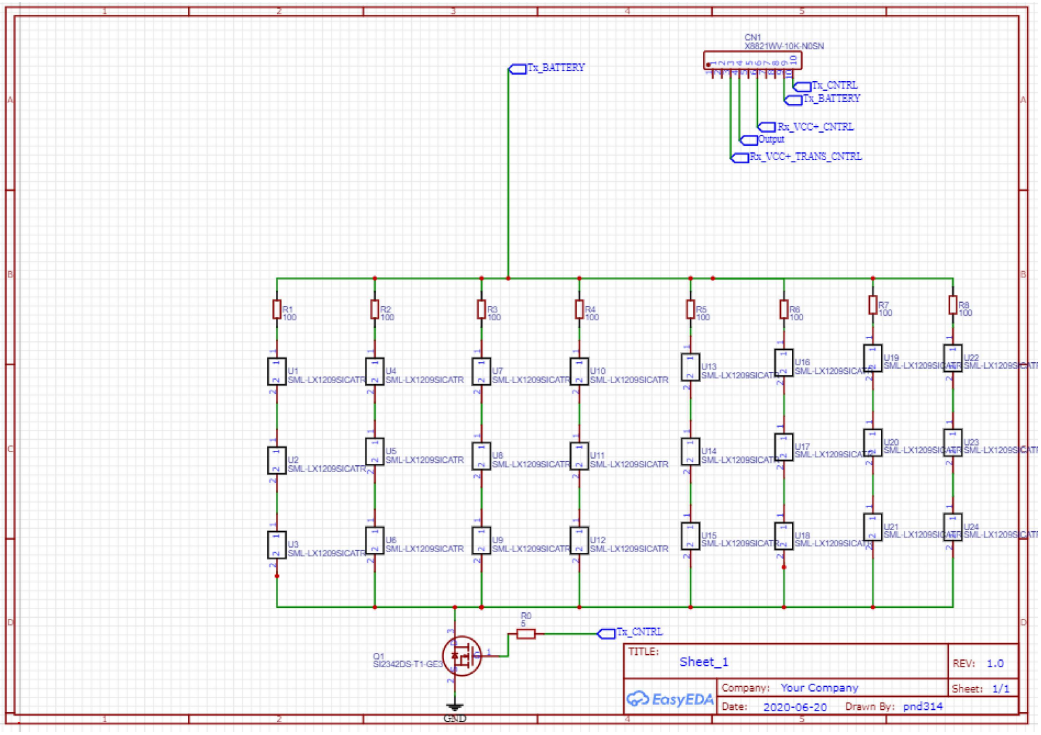

Figure 5. Circuit diagram of the transmit thread.

The switching of the transmit circuit was controlled by using a MOSFET. The signal from the controller which represents the data stream is used as the gate voltage input (Q1) to the MOSFET. This signal effectively controls the current flow through the transmit sources. The output of the MOSFET connects to 24 narrow band

LEDs which are routed in 8 parallel rows of 3 to get balanced current and voltage distribution. Note that the Arduino is there for just routing information, and it is not on the actual board.

4.1.2 Receive Path Schematic

Noting that the design chosen for the prototype was 76 receivers and 24 transmitters, there were several layout combinations to use as the baseline that were reviewed to meet the minimum 76 receiver requirement. Notably, the following were reviewed, although there are many others (resistors vs. path): 13×6, 12×7, 11×7, 11×11, 10×8, 10×10, 9×9, 8×10, 7×11, 6×12. The reason the above were reviewed was because any more paths or more resistors in each path is more easily going to result in an RC delay difference between elements. More importantly, these different receiver layout combinations are just a baseline, as the actual amount chosen can vary depending on requirements of the PCB design. Not all paths need to equal in number of receive elements, and only the total number of the elements on the board must be 76. It is also easier to route elements when there are not too many paths or too many elements per path.

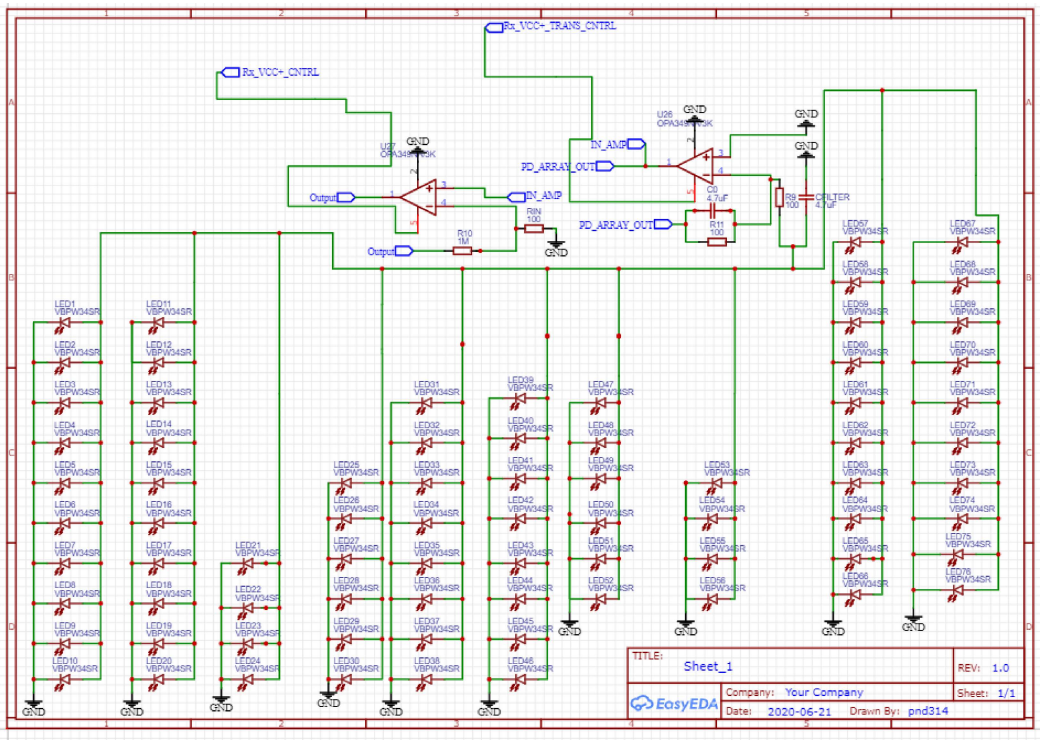

Figure 6. Circuit diagram of the receiver thread.

For this design, the baseline that was chosen was roughly 10×10. The receiver circuit schematic is shown in Fig. 6. This routing path is chosen for mainly three reasons. The first major reason is the amount of rows and columns of the array is a 10×10 array with 76 of the elements being receivers. It is easier for routing to one path per column, with more or less elements per path as needed to match the array. The second reason is the RC delay the elements may impose on the received signal. For a small design with only 76 elements and the size of the board being roughly only 5 inches, the delay the trace length is negligible. However, allowing multiple path to dissipate the accumulated charges for the receiver elements ensures each bit is received without any residual charges in the circuit. The third reason is the overall capacitance of the circuit. For a design with 76 elements, we are dealing with low power, and mostly high DC low AC outputs from the photodiodes. Each photodiode having an individual input on its path would mean all the capacitance in each photodiode directly sums up since each path is seen as parallel, which leads to RC delay. But if we combine the components in series and parallel combination, we can control the effective capacitance of the receiver circuit.

Once the signal is received, as a typical practice in optoelectronic receivers, two stage trans-impedance amplifier is used to convert the photocurrent into voltage level which is stored in the memory of the controller. The internal clock of the controller is used to sample the voltage level of each bit and convert the signal using Analog to Digital Converter (ADC) to reconstruct each bit.

5. CONCLUSION

With the ever increasing data demand for mobile nodes and applications, FSOC provides an alternate solution to the RF infrastructure. A major advantage of FSO ad-hoc networks is the established fiber optic backhaul network, which provides the required high data stream that would match the speed of FSO links to be deployed at the last mile. However, implementation of full-duplex FSO network is challenging for several disadvantages, such as free-space attenuation, transmit power limitation, and mobility. At one hand, FSO enables secure communication due to its directionality; on the other hand, it makes it harder to maintain a stable link for the same reason. In this paper, we outlined a system architecture by designing a multi-element FSO transceiver driver circuit design by considering size, weight, and power (SWaP) constraints for a low-flying drone. We derived a link margin analysis model, which includes free-space attenuation, weather conditions in terms of visibility, SWaP, and system parameters such as bit rate and bandwidth; and determined the link margin for a multi-element transceiver based system. For a 10×10 array transceiver layout, which included 24 transmitters each having transmit power (P_t) of 75 mW and 76 receivers, the link margin of the FSO system is calculated to be 4.82 dB for a system bit rate of 1 Mbps. We also outlined different circuit routing limitations and considerations to optimize the system performance while maintaining SWaP constraints. This design and prototype can be useful for many applications, such as aerial node communication, rescue missions at remote locations, and local surveillance. This work is a part of an ongoing project, which includes prototype implementation and system integration with aerial nodes.

ACKNOWLEDGMENTS

This work is partly supported by National Science Foundation (NSF) award 16226A19.

REFERENCES

[1] Khan, M., Yuksel, M., and Winkelmaier, G., "GPS-free maintenance of a free-space-optical link between two autonomous mobiles," *IEEE Transactions on Mobile Computing* **16**(6), 1644–1657 (2017).

[2] Oh, C. W. J., Cao, Z., Tangdiongga, E., and Koonen, T., "10 Gbps all-optical full-duplex indoor optical wireless communication with wavelength reuse," in [*OFC*], Th4A–6, Optical Society of America (2016).

[3] Haq, A. F. M. S. and Yuksel, M., "Weather-limited in-band full-duplex transceiver model for free-space optical communication," *Optical Engineering* **59**(5), 056113 (2020).

[4] Haq, A. F. M. S., Khan, M. R., and Yuksel, M., "A prototype of in-band full-duplex free-space optical transceiver," in [*2018 IEEE International Symposium on Local and Metropolitan Area Networks (LANMAN)*], 112–113, IEEE (2018).

[5] Haq, A. F. M. S. and Yuksel, M., "Weather limited short-range in-band full-duplex free-space optical transceiver," in [*Free-Space Laser Communications XXXI*], **10910**, 1091021, International Society for Optics and Photonics (2019).

[6] Ryer, A., [*Light Measurement Handbook*], International Light Inc., 17 Graf Road Newburyport, MA 01950 (1997).

[7] Kaymak, Y., Rojas-Cessa, R., Feng, J., Ansari, N., Zhou, M., and Zhang, T., "A survey on acquisition, tracking, and pointing mechanisms for mobile free-space optical communications," *IEEE Communications Surveys & Tutorials* **20**(2), 1104–1123 (2018).

[8] Khan, M., Bhunia, S., Yuksel, M., and Kane, L. C., "Line-of-sight discovery in 3D using highly directional transceivers," *IEEE Transactions on Mobile Computing* **18**(12), 2885–2898 (2018).

[9] Grami, A., [*Introduction to digital communications*], Academic Press (2015).

[10] Kaadan, A., Refai, H. H., and LoPresti, P. G., "Multielement FSO transceivers alignment for inter-UAV communications," *Journal of Lightwave Technology* **32**(24), 4785–4795 (2014).

[11] Eroğlu, Y. S., Güvenç, I., Şahin, A., Yapıcı, Y., Pala, N., and Yuksel, M., "Multi-element VLC networks: LED assignment, power control, and optimum combining," *IEEE Journal on Selected Areas in Communications* **36**(1), 121–135 (2017).

[12] Sabban, A., [*Wideband RF Technologies and Antennas in Microwave Frequencies*], John Wiley and Sons, Inc., Hoboken, New Jersey (2016).

[13] Alexander, S., [*Optical Communication Receiver Design*], SPIE-The International Society for Optical Engineering, P.O Box 10 Bellingham, Washington 98227-0010 (1997).

[14] National Radio Astronomy Observatory, "Antenna fundamentals." https://www.cv.nrao.edu/course/astr534/AntennaTheory.html (2010).

[15] Anis, A., Rahman, A., Rashidi, C., and Aljunid, S., "Link budget analysis for free space optical (FSO) communication under haze condition with adverse wavelength," in [*2016 3rd International Conference on Electronic Design (ICED)*], 354–357, IEEE (2016).

[16] Layne, D., "Receiver sensitivity and equivalent noise bandwidth," *High Frequency Electronics Magazine* , 22 (2014).